

Electric-Field Modulation of Thermopower for the KTaO_3 Field Effect Transistors

Akira Yoshikawa¹, Kosuke Uchida¹, Kunihito Koumoto¹, Takeharu Kato², Yuichi Ikuhara^{2,3}, and Hiromichi Ohta^{1,4*}

¹*Graduate School of Engineering, Nagoya University, Furo, Chikusa, Nagoya 464-8603, Japan*

²*Japan Fine Ceramics Center, 2-4-1 Mutsuno, Atsuta, Nagoya 456-8587, Japan*

³*Institute of Engineering Innovation, The University of Tokyo, 2-11-16 Yayoi, Bunkyo, Tokyo 113-8656, Japan*

⁴*PRESTO, Japan Science and Technology Agency, Honcho, Kawaguchi, Saitama 332-0012, Japan*

*E-mail address: h-ohta@apchem.nagoya-u.ac.jp

We show herein fabrication and field-modulated thermopower for KTaO_3 single-crystal based field-effect transistors (FETs). The KTaO_3 FET exhibits field effect mobility of $\sim 8 \text{ cm}^2 \text{ V}^{-1} \text{ s}^{-1}$, which is ~ 4 times larger than that of SrTiO_3 FETs. The thermopower of the KTaO_3 FET decreased from 600 to 220 μVK^{-1} by the application of gate electric field up to 1.5 MVcm^{-1} , $\sim 400 \mu\text{VK}^{-1}$ below that of an SrTiO_3 FET, clearly reflecting the smaller carrier effective mass of KTaO_3 .

Thermoelectric energy conversion technology attracts attention to convert the waste heat into electricity.¹⁾ Generally, the performance of thermoelectric materials is evaluated in terms of a dimensionless figure of merit, $ZT = S^2 \cdot \sigma T \cdot \kappa^{-1}$, where Z , T , S , σ and κ are a figure of merit, the absolute temperature, the thermopower, the electrical conductivity, and the thermal conductivity, respectively. Today, thermoelectric materials with $ZT > 1$, which is necessary for practical applications, are being rigorously explored, mostly using charge carrier-doped semiconductors with various doping levels because the $S^2 \cdot \sigma$ value must be enhanced according to the commonly observed trade-off relationship between two material parameters in terms of charge carrier concentration (n): σ increases almost linearly with increasing n until ionized impurity scattering or electron-electron scattering becomes dominant, while $|S|$ decreases with n . Therefore, a number of materials are usually needed to optimize thermoelectric properties.

Very recently, Sakai *et al.*²⁾ reported thermoelectric properties of several Ba-doped KTaO_3 single crystals ($n = 5.4 \times 10^{18} - 1.4 \times 10^{20} \text{ cm}^{-3}$). They found that heavy ($>10^{20} \text{ cm}^{-3}$) electron doping in KTaO_3 would provide large thermoelectric properties. KTaO_3 (S.G.: $Pm3m$, lattice parameter $a = 3.989 \text{ \AA}$) is a typical band insulator with a large band gap of $\sim 3.8 \text{ eV}$.³⁾ Metallic conductivity in KTaO_3 can be obtained by the appropriate impurity doping⁴⁾ and/or the introduction of oxygen vacancies.⁵⁻⁷⁾ KTaO_3 exhibits very high Hall mobility of $>10^4 \text{ cm}^2 \text{V}^{-1} \text{s}^{-1}$ at 2 K.⁸⁾ Since these physical properties of KTaO_3 are similar to those of SrTiO_3 ,^{9,10)} which exhibits largest ZT among transition metal oxides (n -type), KTaO_3 would be promising candidate for thermoelectric application.

In order to examine the thermoelectric properties of S and σ for KTaO_3 , we fabricated a field effect transistor (FET) structure on a single crystal KTaO_3 because a

FET structure on single-crystalline material would be a powerful tool in optimizing thermoelectric properties because it provides the charge carrier dependence of both S - and σ -values simultaneously.¹¹⁾ The resultant KTaO_3 FET exhibits following transistor characteristics: on-off current ratio of $\sim 10^5$, sub-threshold swing S-factor of 1.2 Vdecade^{-1} , threshold gate voltage V_{th} of $+5.2 \text{ V}$, and field effect mobility μ_{FE} of $\sim 8 \text{ cm}^2\text{V}^{-1}\text{s}^{-1}$. The thermopower $|S|$ of this KTaO_3 FET can be modulated from 600 to $220 \mu\text{VK}^{-1}$ by the application of gate electric field up to 1.5 MVcm^{-1} .

Here we report the fabrication and thermopower modulation of the KTaO_3 FET. The schematic structure and photograph of the KTaO_3 FET are shown in Figs. 1(a) and 1(b), respectively. First, we treated (001) KTaO_3 single crystal plates ($10 \times 10 \times 0.5 \text{ mm}$, SHINKOSHA) with buffered NH_4F -HF solution (BHF, $\text{pH} = 4.5$) to obtain an atomically smooth surface¹²⁾ because atomically smooth heterointerface of the gate insulator/oxide may be necessary for FET fabrication.¹³⁾ The NH_4F concentration was kept at 10 mol/l . After the BHF treatment, we obtained a relatively smooth surface with steps ($\sim 0.4 \text{ nm}$) and terraces [Fig. 2(b)] as compared to an untreated surface [Fig. 2(a)]. Second, 20-nm-thick metallic Ti films, which would serve as source and drain electrodes, were deposited onto the stepped KTaO_3 surface by electron beam (EB, no substrate heating, base pressure $\sim 10^{-4} \text{ Pa}$) evaporation through a stencil mask. Third, 200-nm-thick amorphous $12\text{CaO}\cdot 7\text{Al}_2\text{O}_3$ ($a\text{-C12A7}$, permittivity $\epsilon_r = 12$) glass film was deposited by a pulsed laser deposition (PLD, $\sim 3 \text{ Jcm}^{-2}\text{pulse}^{-1}$, oxygen pressure $\sim 0.1 \text{ Pa}$) at room temperature (RT, no substrate heating). It should be noted that $a\text{-C12A7}$ glass would be an appropriate gate insulator for SrTiO_3 and KTaO_3 as compared to $a\text{-Al}_2\text{O}_3$.^{13,14)} Finally, a 20-nm Ti film was deposited by EB evaporation as described above. In order to reduce the off current, the FETs were annealed at $150 \text{ }^\circ\text{C}$ in air.

Figure 2(c) shows a cross-sectional high-resolution transmission electron microscope image of the a -C12A7/KTaO₃ interface region (HRTEM, TOPCON EM-002B, acceleration voltage 200 kV, TOPCON). The featureless a -C12A7 (upper part) is observed, although the KTaO₃ layer exhibits a lattice (lower part). A broad halo is seen in the selected area electron diffraction patterns of a -C12A7, indicating that amorphous a -C12A7 film was deposited on the KTaO₃ layer.

Transistor characteristics of the resultant KTaO₃ FETs were measured by using a semiconductor device analyzer (B1500A, Agilent Technologies) at RT. The channel width (W) and the channel length (L) of the FET were 400 and 200 μm , respectively. Figure 3 summarizes typical transistor characteristics, such as transfer characteristics, field-effect mobility, sheet charge concentration, and the output of these FETs. The drain current (I_d) of the KTaO₃ FET increased markedly as the gate voltage (V_g) increased, hence the channel was n -type, and electron carriers were accumulated by positive V_g [Fig. 3(a)]. Relatively large hysteresis (~ 1 V) in I_d was also observed, most likely due to traps ($\sim 10^{12}$ cm⁻²) at the a -C12A7/KTaO₃ interface. The on-off current ratio and the S-factor were $>10^5$ and ~ 1.2 V·decade⁻¹, respectively. The threshold gate voltage (V_{th}), obtained from a linear fit of the $I_d^{0.5}$ - V_g plot [Fig. 3(b)], was +5.2 V.

Using the above measured values, we calculated the sheet charge concentration (n_{xx}) and the field-effect mobility (μ_{FE}) of the KTaO₃ FETs. The n_{xx} values were obtained from $n_{xx} = C_i (V_g - V_{th})$, where C_i was the capacitance per unit area (51 nFcm⁻²). The μ_{FE} values were obtained from $\mu_{FE} = g_m [(W/L)C_i \cdot V_d]^{-1}$, where g_m was the transconductance $\partial I_d / \partial V_g$. As shown in Fig. 3(c), μ_{FE} of the FET increased drastically with V_g and reached ~ 8 cm²V⁻¹s⁻¹, which is $\sim 25\%$ of the RT Hall mobility of electron-doped KTaO₃ ($\mu_{Hall} \sim 30$ cm²V⁻¹s⁻¹). We also note that μ_{FE} of the KTaO₃ FETs

were a factor of 4 greater than those of SrTiO₃ FETs,¹¹⁾ most likely due to the difference in effective mass of the charge carrier m_e^* (KTaO₃: 0.13 m_0 , SrTiO₃: 1.16 m_0). Furthermore, we observed a clear pinch-off and current saturation in I_d [Fig. 3(d)], indicating that the operation of this FET conformed to standard FET theory.

Then, we measured field-modulated thermopower (S_{FE}) of the KTaO₃ FET. First, a temperature difference ($\Delta T = 0.2\text{--}1.5$ K) was introduced between the source and drain electrodes by using two Peltier devices. Then, thermo-electromotive force (V_{TEMF}), which is the open circuit voltage between the source and the drain electrodes, was measured during the V_g -sweeping. The values of S were obtained from the slope of $V_{TEMF}\text{--}\Delta T$ plots (data not shown). Figure 4 shows $S_{FE}\text{--}V_g$ plots for the KTaO₃ FETs. The S_{FE} -values are negative, confirming that the channel is n -type. $|S|_{FE}$ gradually decreases from 600 to 220 μVK^{-1} by the application of gate electric field up to 1.5 MVcm^{-1} , due to the fact that n_{xx} increases with the V_g increases. These $|S|_{FE}$ values are approximately 400 μVK^{-1} lower than those for a SrTiO₃ FET as shown in the inset.¹¹⁾ Since the value of $|S|_{FE}$ strongly depends on m_e^* ,¹⁶⁾ this result reflects the fact that m_e^* of KTaO₃ (0.13 m_0) is lower than that of SrTiO₃ (1.16 m_0).

In summary, we have fabricated single crystal KTaO₃-based field-effect transistors using amorphous 12CaO·7Al₂O₃ glass gate insulator. The resultant FET exhibit following characteristics: on-off current ratio of $\sim 10^5$, sub-threshold swing S-factor of 1.2 Vdecade^{-1} , threshold gate voltage V_{th} of +5.2 V, and field effect mobility μ_{FE} of $\sim 8 \text{ cm}^2\text{V}^{-1}\text{s}^{-1}$ (a factor of 4 greater than for SrTiO₃ FETs). The observed values of thermopower for the KTaO₃ FETs were $\sim 400 \mu\text{VK}^{-1}$ below those of SrTiO₃ FETs, clearly demonstrating the difference of carrier effective mass m_e^* (KTaO₃: 0.13 m_0 , SrTiO₃: 1.16 m_0).

Acknowledgement A part of this work was financially supported by Ministry of Education, Culture, Sports, Science and Technology (Nano Materials Science for Atomic-scale Modification, 20047007).

References

- [1] T. M. Tritt, M. A. Subramanian, H. Bottner, T. Caillat, G. Chen, R. Funahashi, X. Ji, M. Kanatzidis, K. Koumoto, G. S. Nolas, J. Poon, A. M. Rao, I. Terasaki, R. Venkatasubramanian, and J. Yang: MRS Bull. (special issue on harvesting energy through thermoelectrics: power generation and cooling) **31** (2006) 188 and articles therein.
- [2] A. Sakai, T. Kanno, S. Yotsuhashi, H. Adachi, and Y. Tokura: Jpn. J. Appl. Phys. **48** (2009) 097002.
- [3] W. S. Baer: J. Phys. Chem. Solids **28** (1967) 677.
- [4] W. R. Hosler and H. P. R. Frederikse: Solid State Commun. **7** (1969) 1443.
- [5] M. Tsukioka, J. Tanaka, and Y. Miyazawa: J. Phys. Soc. Jpn. **46** (1979) 1785.
- [6] G. O. Deputy, and R. W. Vest: J. Am. Ceram. Soc. **61** (1978) 321.
- [7] V. F. Shamrai, A. V. Arakcheeva, V. V. Grinevich, and A. B. Mikhailova: Crystallogr Rep+. **50** (2004) 779.
- [8] S. H. Wemple: Phys. Rev. A **137** (1965) 1575.
- [9] O. N. Tufte and P. W. Chapman: Phys. Rev. **155** (1967) 796.
- [10] H. P. R. Frederikse, W. R. Thurber, and W. R. Hosler: Phys. Rev. **134** (1964) A442.
- [11] H. Ohta, Y. Masuoka, R. Asahi, T. Kato, Y. Ikuhara, K. Nomura, and H. Hosono: Appl. Phys. Lett. **95** (2009) 113505.
- [12] M. Kawasaki, K. Takahashi, T. Maeda, R. Tsuchiya, M. Shinohara, O. Ishiyama, T. Yonezawa, M. Yoshimoto, and H. Koinuma: Science **266** (1994) 1540.
- [13] K. Ueno, I. H. Inoue, T. Yamada, H. Akoh, Y. Tokura, and H. Takagi, Appl. Phys. Lett. **84** (2004) 3726.
- [14] K. Ueno, I. H. Inoue, H. Akoh, M. Kawasaki, Y. Tokura, and H. Takagi: Appl. Phys.

Lett. **83** (2003) 1755.

[15] H. Ohta, K. Sugiura, and K. Koumoto: *Inorg. Chem.* **47** (2008) 8429.

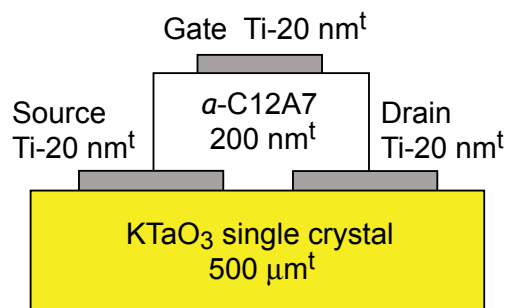
[16] C. B. Vining: *J. Appl. Phys.* **69** (1991) 331.

Figure 1 (a) The schematic device structure and (b) a photograph of the KTaO_3 FET. Ti films (20-nm-thick) are used as the source, drain and gate electrodes. A 200-nm-thick α -C12A7 film is used as the gate insulator. Channel length (L) and channel width (W) are 200 and 400 μm , respectively.

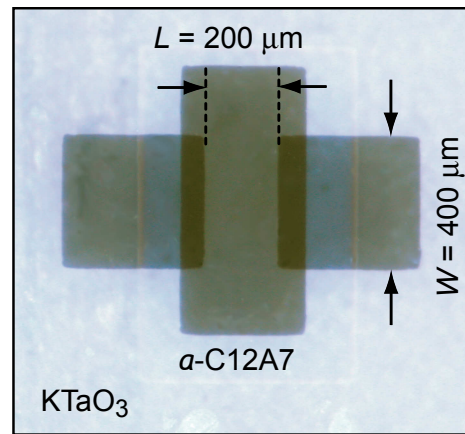
Figure 2 Topographic AFM images of (a) untreated and (b) BHF-treated KTaO_3 single-crystal surface. A smooth surface with steps and terraces is observed in (b). (c) Cross-sectional HRTEM image of the 200-nm-thick α -C12A7/ KTaO_3 heterointerface.

Figure 3 Typical transistor characteristics of a KTaO_3 FET with 200-nm-thick α -C12A7 ($\epsilon_r = 12$) gate insulator at RT [(a) Transfer characteristic ($I_d - V_g$ plot), (b) $I_d^{0.5} - V_g$ plot, (c) field-effect mobility (μ_{FE})-sheet charge density (n_{xx}) - V_g plots, (d) Output characteristic ($I_d - V_d$ plot)].

Figure 4 Field-modulated thermopower (S) for the KTaO_3 FET channel. S for the SrTiO_3 FET channel¹¹⁾ is also plotted in the inset for comparison. Thermopower $|S|$ of the KTaO_3 FET is roughly $\sim 400 \mu\text{VK}^{-1}$ smaller than that of SrTiO_3 FET and can be tuned from 600 to 220 μVK^{-1} .



(a)



(b)

Figure 1

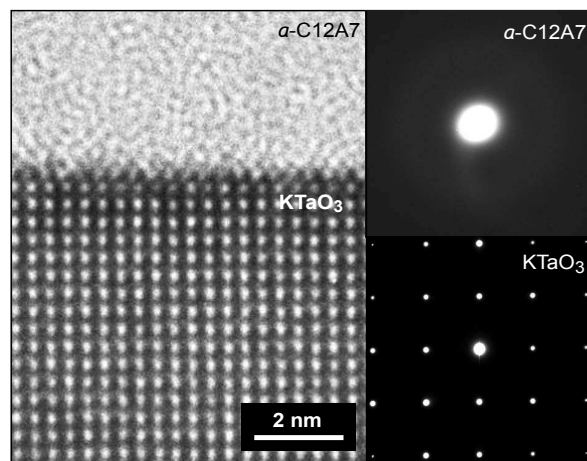
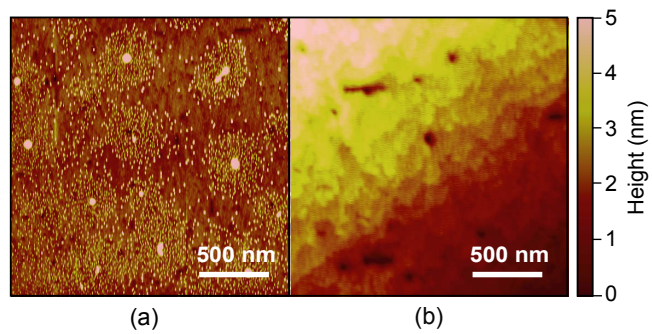


Figure 2

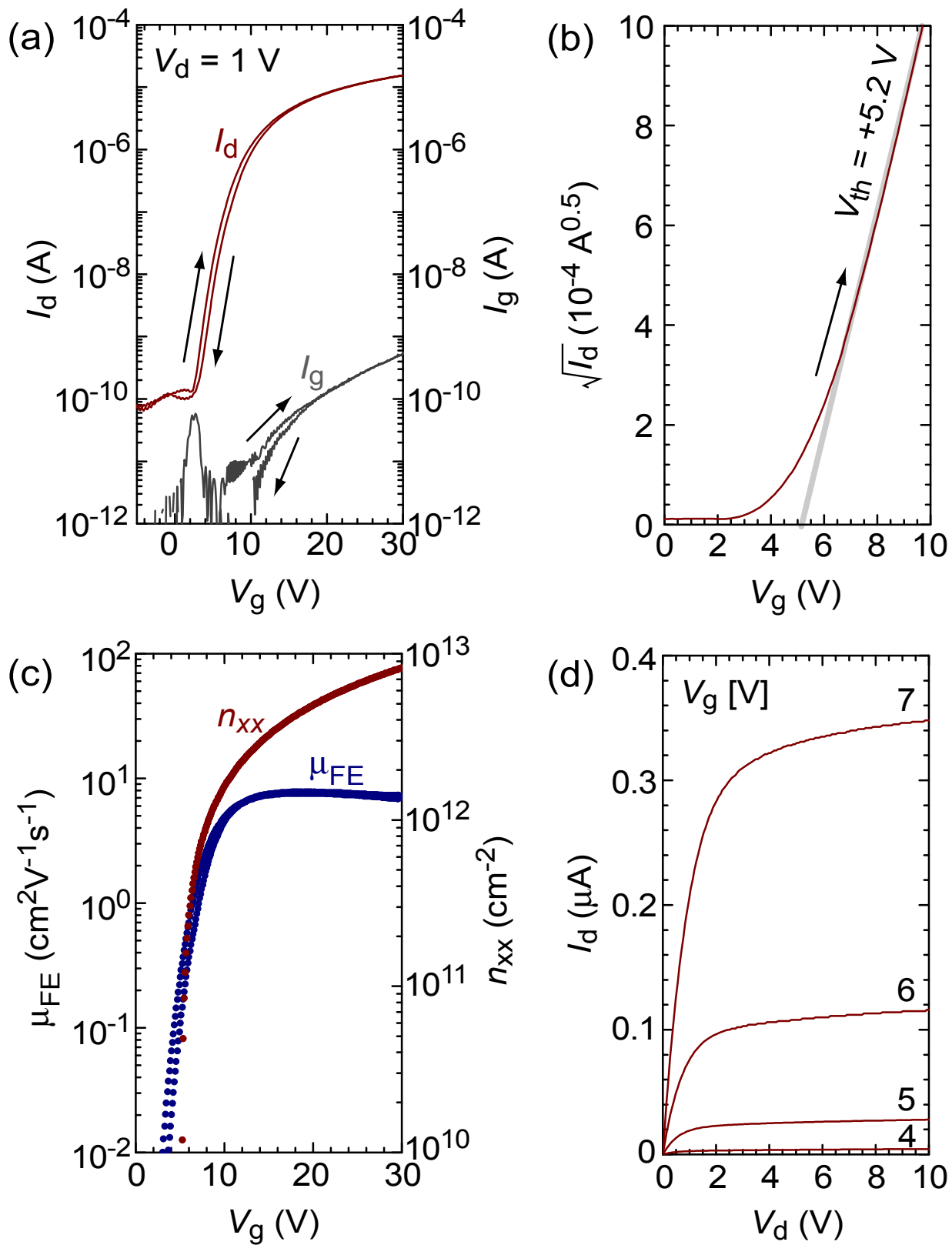


Figure 3

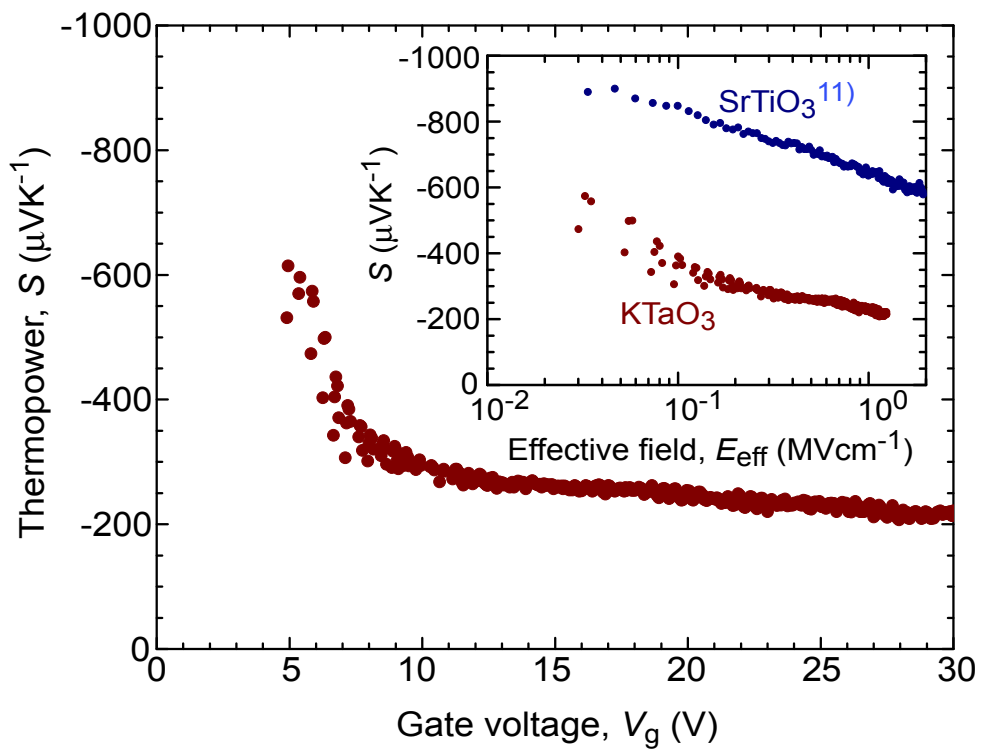


Figure 4